Pauli-limited upper critical field of Fe$_{1+y}$Te$_{1-x}$Se$_x$

Hechang Lei (雷和畅),[1] Rongwei Hu (胡荣伟),[1,*] E. S. Choi,[2] J. B. Warren,[3] and C. Petrovic[1]

[1]*Condensed Matter Physics and Materials Science Department, Brookhaven National Laboratory, Upton, New York 11973, USA*
[2]*NHMFL/Physics, Florida State University, Tallahassee, Florida 32310, USA*
[3]*Instrumentation Division, Brookhaven National Laboratory, Upton, New York 11973, USA*

In this work, we investigated the temperature dependence of the upper critical field $\mu_0 H_{c2}(T)$ of Fe$_{1.02(3)}$Te$_{0.61(4)}$Se$_{0.39(4)}$ and Fe$_{1.05(3)}$Te$_{0.89(2)}$Se$_{0.11(2)}$ single crystals by measuring the magnetotransport properties in stable dc magnetic fields up to 35 T. Both crystals show that $\mu_0 H_{c2}(T)$ in the ab plane and along the c-axis exhibit saturation at low temperatures. The anisotropy of $\mu_0 H_{c2}(T)$ decreases with decreasing temperature, becoming nearly isotropic when the temperature $T \to 0$. Furthermore, $\mu_0 H_{c2}(0)$ deviates from the conventional Werthamer-Helfand-Hohenberg theoretical prediction values for both field directions. Our analysis indicates that the spin-paramagnetic pair-breaking effect is responsible for the temperature-dependent behavior of $\mu_0 H_{c2}(T)$ in both field directions.

I. INTRODUCTION

The discovery of superconductivity in REOFePn (RE =rare earth; Pn=P or As, 1111-system)[1–5] with high-transition temperature T_c has generated a great deal of interests. Shortly after, several other groups of iron-based superconductors have been discovered, such as AFe$_2$As$_2$ (A =alkaline or alkaline-earth metals, 122-system),[6,7] LiFeAs (111-system),[8] (Sr$_4M_2$O$_6$)(Fe$_2$Pn$_2$) (M=Sc, Ti, or V, 42622-system),[9,10] and α-PbO type FeSe (11-system).[11] In particular, the discovery of superconductivity in FeSe, FeTe$_{1-x}$Se$_x$,[12] and FeTe$_{1-x}$S$_x$ (Ref. 13) opened new directions. Simple binary Fe based superconductors can help to understand the mechanism of superconductivity because they share the most prominent characteristics with other iron-based superconductors, i.e., a square-planar lattice of Fe with tetrahedral coordination and similar Fermi surface topology.[14] Furthermore, 11-type superconductors exhibit some distinctive features: absence of charge reservoir, significant pressure effect,[15] and excess Fe with local moment.[16]

In order to understand the mechanism of superconductivity of iron-based superconductors, it is important to study the upper critical field $\mu_0 H_{c2}$. This is one of the most important superconducting parameters since it provides valuable information on fundamental superconducting properties: coherence length, anisotropy, details of underlying electronic structures, and dimensionality of superconductivity as well as insights into the pair-breaking mechanism.

There are two remarkable common characteristics in $\mu_0 H_{c2}$-T phase diagram in iron-based superconductors. For 1111-system, $\mu_0 H_{c2,c}(T)$ shows pronounced upturn curvature at low temperatures. In contrast, $\mu_0 H_{c2,ab}(T)$ exhibits a downturn curvature with decreasing temperature.[17] The former can be explained by two band theory with high-diffusivity ratio of electron band to hole band and the latter is mainly ascribed to the spin-paramagnetic effect.[17–19] For 122-system [(Ba,K)Fe$_2$As$_2$ and Sr(Fe,Co)$_2$As$_2$], the upturn curvature of $\mu_0 H_{c2,c}(T)$ present in 1111-system does not appear, but it still shows positive curvature of temperature far below T$_c$ without saturation.[20–22] It can also be interpreted

using two band theory with smaller diffusivity ratio of two bands when compared to 1111-system.[21] On the other hand $\mu_0 H_{c2,ab}(T)$ tends to saturate with decreasing temperature and it also originates from spin-paramagnetic effect.[23] However, for KFe$_2$As$_2$, both $\mu_0 H_{c2,ab}(T)$ and $\mu_0 H_{c2,c}(T)$ show saturation trend at low temperature with different negative curvature. The former can be ascribed to the spin-paramagnetic effect and the latter is mainly determined by orbital limited field in one band scenario.[24]

Previous research on polycrystalline FeSe$_{0.25}$Te$_{0.75}$ using pulsed magnetic fields up to 55 T, indicated that spin-paramagnetic effect dominates $\mu_0 H_{c2}(T)$.[25] However, it is necessary to elucidate whether this kind of effect dominates the $\mu_0 H_{c2,ab}(T)$ or (and) $\mu_0 H_{c2,c}(T)$. In this work, we report the upper critical field anisotropy of Fe$_{1.02(3)}$Te$_{0.61(4)}$Se$_{0.39(4)}$ and Fe$_{1.05(3)}$Te$_{0.89(2)}$Se$_{0.11(2)}$ single crystals in stable dc high magnetic field up to 35 T. We show that spin-paramagnetic effect is dominant in both of $\mu_0 H_{c2,ab}(T)$ and $\mu_0 H_{c2,c}(T)$.

II. EXPERIMENT

Single crystals of Fe(Te,Se) were grown by self-flux method with nominal composition FeTe$_{0.5}$Se$_{0.5}$ and FeTe$_{0.9}$Se$_{0.1}$. Stoichiometric elemental Fe (purity 99.98%, Alfa Aesar), Te (purity 99.999%, Alfa Aesar), and Se (purity 99.999%, Alfa Aesar) were sealed in quartz tubes under partial argon atmosphere. The sealed ampoule was heated to a soaking temperature of 950 °C, then slowly cooled to 300–400 °C. Platelike crystals up to $2 \times 5 \times 1$ mm^3 can be grown. The powder x-ray diffraction (XRD) spectra were taken with Cu K$_\alpha$ radiation (λ=1.5418 Å) using a Rigaku miniflex x-ray machine. XRD results of the ground samples indicate the phases for both of them are pure. The lattice parameters, a=b=3.798(2) Å, c=6.063(2) Å and a=b =3.818(2) Å, c=6.243(2) Å for nominal composition FeTe$_{0.5}$Se$_{0.5}$ and FeTe$_{0.9}$Se$_{0.1}$, respectively, are obtained by fitting the XRD spectra using the RIETICA software.[26] On the other hand, XRD spectra of single crystals reveal that the crystal surface is normal to the c-axis with the plate-shaped surface parallel to the ab-plane. The elemental and micro-
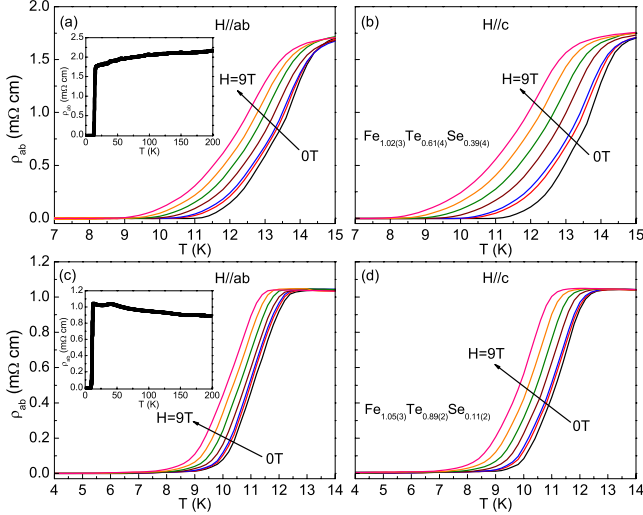
FIG. 1. (Color online) Temperature dependence of the resistivity $\rho_{ab}(T)$ of Se-39 for (a) $H\|ab$ and (b) $H\|c$ of Se-39 and of Se-11 for (c) $H\|ab$ and (d) $H\|c$ at the various magnetic fields from 0 to 9 T (0, 0.5, 1, 3, 5, 7, and 9 T). Insets of (a) and (c) show the resistivity of Se-39 and Se-11 at the temperature range of 1.8–200 K, respectively.

structure analysis were performed using energy-dispersive x-ray spectroscopy in an JEOL JSM-6500 scanning electron microscope. The average stoichiometry was determined by examination of multiple points on the crystals. The measured compositions are $Fe_{1.02(3)}Te_{0.61(4)}Se_{0.39(4)}$ and $Fe_{1.05(3)}Te_{0.89(2)}Se_{0.11(2)}$. They will be denoted as Se-39 and Se-11 in the following for brevity. Electrical transport measurements were performed using a four-probe configuration on rectangular shaped polished single crystals with current flowing in *ab*-plane of tetragonal structure. Thin Pt wires were attached to electrical contacts made of Epotek H20E silver epoxy. Sample dimensions were measured with an optical microscope Nikon SMZ-800 with 10 μm resolution. Electrical transport measurements were carried out in dc fields up to 9 T in a quantum design PPMS-9 from 1.8 to 200 K and up to 35 T in a resistive magnet in a He3 cryostat down to 0.3 K at the National High Magnetic Field Laboratory (NHMFL) in Tallahassee, Florida.

III. RESULTS

Temperature-dependent resistivity of $\rho_{ab}(T)$ of Se-39 and Se-11 below 15 K in low magnetic fields from 0 to 9 T for $H\|ab$ and $H\|c$ are shown in Fig. 1. With increasing magnetic fields, the resistivity transition width becomes slightly broader and the onset of superconductivity gradually shifts to lower temperatures. The trend is more pronounced for $H\|c$ than $H\|ab$. This is similar to previous reports for Fe(Te,S) and FeTe$_{0.7}$Se$_{0.3}$ single crystals.[27,28] It is worth noting that the shape and width of $\rho_{ab}(T)$ broadening with $H\|c$ is comparable to that of the 122-system, e.g., the single crystal of (Ba,K)Fe$_2$As$_2$ and (Ba,Rb)Fe$_2$As$_2$.[29,30] It is rather different from 1111-system such as single crystal of SmO$_{0.7}$F$_{0.25}$FeAs and SmO$_{0.85}$FeAs.[19,31] Similar field broadening of resistivity
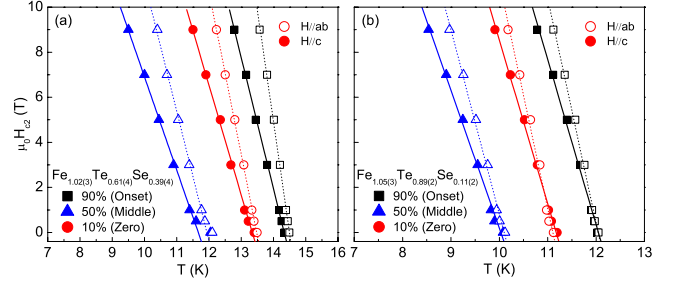
FIG. 2. (Color online) Temperature dependence of the resistive upper critical field $\mu_0 H_{c2}(T)$ of (a) Se-39 and (b) Se-11 corresponding three defined temperatures at low fields. The dotted and solid lines are linear fitting to the data for $H\|c$ and $H\|ab$, respectively.

of the 1111-system with $H\|c$ was also observed in cuprates.[32–34] and explained by the vortex-liquid state.[35] Recent report on NdFeAsO$_{1-x}$F$_x$ single crystals confirmed the existence of the vortex-liquid state in 1111-system.[36] Hence, the vortex-liquid state region is narrower even absent in Fe-(Te,Se) (11-system).

Insets of Figs. 1(a) and 1(c) show the temperature dependence of the resistivity $\rho_{ab}(T)$ for Se-39 and Se-11 at zero field from 1.8 to 200 K. Both undergo a relatively sharp superconducting transition at $T_{c,\text{onset}}=14.4$ and 12 K for Se-39 and Se-11, respectively. It should be noted that, as seen from the insets, Se-39 exhibits a metallic resistivity behavior in normal state, whereas Se-11 is not metallic. This difference can be ascribed to different Se content.[12,37] The non-metallic behavior of Se-11 has also been observed in low S doped FeTe single crystals.[27] In addition, more excess Fe in Fe(2) site for Se-11 than Se-39 could lead to weak charge carrier localization.[28,38] On the other hand, there is an anomalous peak in $\rho_{ab}(T)$ for Se-11 at $T \simeq 42$ K. It corresponds to simultaneous structural and (or) antiferromagnetic transitions. Comparing with undoped FeTe,[39] the transition has been depressed from around 65–42 K.

Figure 2 shows the upper critical field $\mu_0 H_{c2}(T)$ of Se-39 and Se-11 corresponding to the temperatures where the resistivity drops to 90% of the normal state resistivity $\rho_{n,ab}(T,H)(T_{c,\text{onset}})$, 50% of $\rho_{n,ab}(T,H)(T_{c,\text{middle}})$ and 10% of $\rho_n(T,H)(T_{c,\text{zero}})$ in low fields. The normal-state resistivity $\rho_{n,ab}(H,T)$ was determined by linearly extrapolating the normal-state behavior above the onset of superconductivity transition in $\rho_{ab}(T)$ curves (same as for $\rho_{ab}(H)$ curves). Because the curves of $\mu_0 H_{c2}(T)$ for all defined temperatures are almost linear except for $\mu_0 H_{c2}(T_{c,\text{zero}})$ of Se-39 with slightly upturn curvature near 0 T, we use the linear fitting results at low field near T_c as the slopes of $\mu_0 H_{c2}(T_c)$. This is shown by solid and dotted lines in Fig. 2 and the values are listed in Table I. According to the conventional one-band Werthamer-Helfand-Hohenberg (WHH) theory, which describes the orbital limited upper critical field of dirty type-II superconductors,[40] the $\mu_0 H^*_{c2}(0)$ can be described by

$$\mu_0 H^*_{c2}(0) = -0.693\left(\frac{d\mu_0 H_{c2}}{dT}\right)_{T_c} T_c, \qquad (1)$$

and the values corresponding to three defined temperatures are also listed in Table I.

TABLE I. $(d\mu_0 H_{c2}/dT)_{Tc}$ and derived $\mu_0 H_{c2}^*(0)$ data at three defined temperatures using WHH formula for Se-39 and Se-11. $\mu_0 H_{c2,ab}^*(0)$ and $\mu_0 H_{c2,c}^*(0)$ are the *ab*-plane and *c*-axis orbital limited upper critical fields at $T=0$ K.

		T_c (K)	$(d\mu_0 H_{c2}/dT)_{Tc}$, $H\|ab$ (T/K)	$(d\mu_0 H_{c2}/dT)_{Tc}$, $H\|c$ (T/K)	$\mu_0 H_{c2,ab}^*(0)$ (T)	$\mu_0 H_{c2,c}^*(0)$ (T)
$Fe_{1.02(3)}Te_{0.61(4)}Se_{0.39(4)}$	Onset	14.4	−9.9	−5.8	98.8	57.9
	Middle	13.4	−7.2	−4.9	66.8	45.5
	Zero	12.1	−5.7	−4.1	47.8	34.4
$Fe_{1.05(3)}Te_{0.89(2)}Se_{0.11(2)}$	Onset	12.0	−10.0	−7.1	83.1	59.0
	Middle	11.2	−10.0	−7.3	77.6	56.7
	Zero	10.1	−8.2	−6.1	57.4	42.7

The magnetic field dependence of resistivity $\rho_{ab}(H)$ of Se-39 and Se-11 are presented in Fig. 3. It can be clearly seen that superconductivity is suppressed by increasing magnetic field at the same temperature and the transition of $\rho_{ab}(H)$ curves are shifted to lower magnetic fields at higher measuring temperature. Comparing with Se-11, the superconductivity of Se-39 still appears under field up to 35 T when temperature is below 1.47 K, indicating Se-39 has a higher $\mu_0 H_{c2}(0)$ than Se-11 in both directions.

Figure 4 shows the temperature dependence of resistivity at high-magnetic fields. For Se-11, the superconductivity above 0.3 K is suppressed at $\mu_0 H=35$ T, irrespective of the direction of field. However, it still survives below 1.5 K for Se-39. This is consistent with the results of $\rho_{ab}(H)$ measurement. The superconducting transition widths of both samples are only slightly broader even at 35 T. It indicates that the vortex-liquid state in Fe(Te,Se) is much narrow or even absent in both low-field high-temperature region and high-field low-temperature region. On the other hand, the $\rho_{ab}(T)$ curves for $H\|c$ and $H\|ab$ approach each other gradually with increasing filed. This trend is more pronounced for Se-11 sample. The anisotropy of upper critical field is decreasing with increasing field.
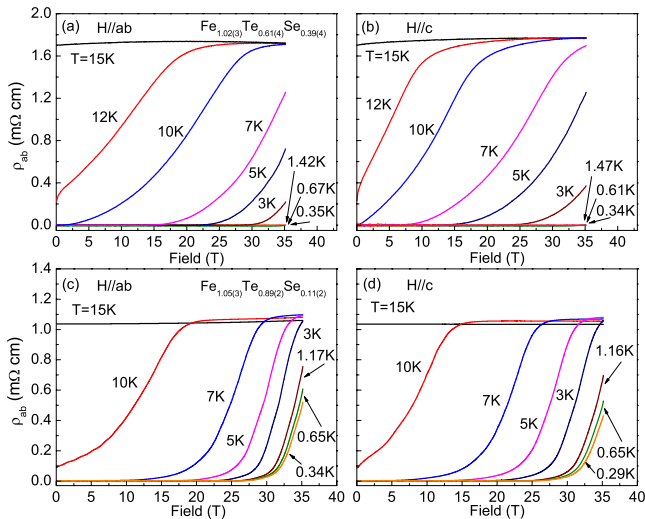
By combining the magnetotransport results in low and high magnetic fields we show phase diagrams in Fig. 5. Both samples show linear increase in $\mu_0 H_{c2}(T)$ with decreasing temperature near T_c. For Se-11 there is a saturation trend at temperatures far below T_c irrespective of field direction. It can also be seen clearly that the $\mu_0 H_{c2}(T)$ of Se-39 is higher than that of Se-11 for both field directions. Data above 35 T were extracted by linear extrapolation of $\rho_{ab}(H)$ at $\mu_0 H < 35$ T to $\rho_{ab}(H)=0.9\rho_{n,ab}(T_c,H)$. The upper critical fields from high-magnetic field measurement are much smaller than those predicted using the conventional WHH model (Table I), especially for $H\|ab$.

IV. DISCUSSION

In what follows, we analyze the possible reasons for the deviation of $\mu_0 H_{c2}(0)$ from the conventional WHH model. Only the $\mu_0 H_{c2,onset}(T)$ were chosen for further analysis.[18,41] In the conventional BCS model, orbital effect arising from the Lorentz force acting on paired electrons with opposite momenta is the main cause of pair breaking. The superconductivity is destroyed when the kinetic energy exceeds the condensation energy of the Cooper pairs. On the other hand, superconductivity can also be eliminated via breaking the singlet pair into unbound triplet. In other words, the Pauli spin susceptibility energy exceeding the condensation energy leads to the partial alignment of the spins. This is spin Zeeman effect, also called spin-paramagnetic effect. The effects of Pauli spin paramagnetism and spin-orbit interaction were included in the WHH theory through the Maki parameters α and λ_{so}.[42] For an isotropic type-II superconductor in the dirty

FIG. 3. (Color online) Field dependence of the resistivity $\rho_{ab}(H)$ of Se-39 for (a) $H\|ab$ and (b) $H\|c$, and of Se-11 for (c) $H\|ab$ and (d) $H\|c$ measured at various temperatures in dc magnetic fields up to 35 T.
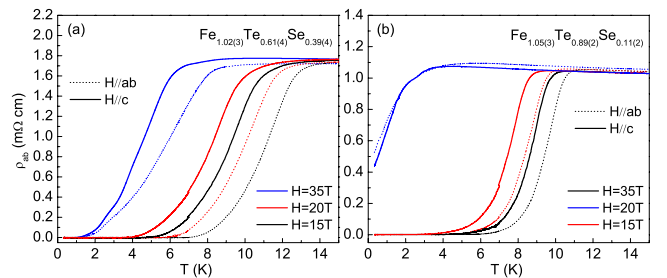
FIG. 4. (Color online) Temperature dependence of the resistivity $\rho_{ab}(T)$ at high-magnetic fields from 15 to 35 T (15, 20, and 35 T) for (a) Se-39 and (b) Se-11.
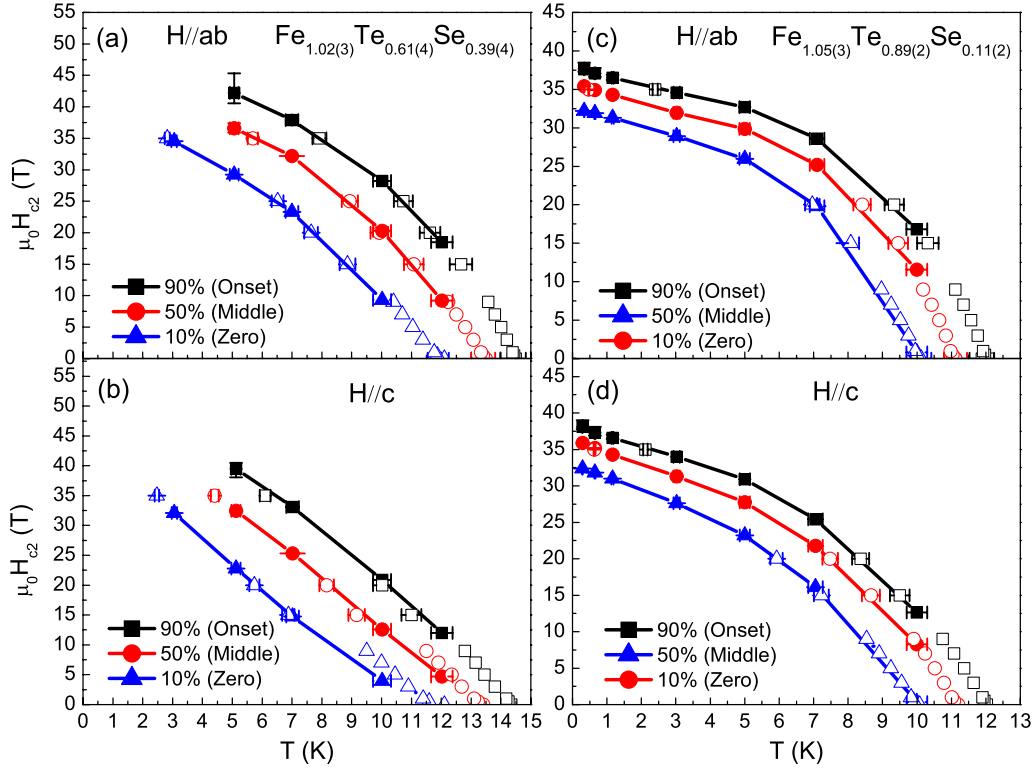
FIG. 5. (Color online) Temperature dependence of the resistive upper critical field $\mu_0 H_{c2}(T)$ of Se-39 for (a) $H\|ab$ and (b) $H\|c$ and of Se-11 for (c) $H\|ab$ and (d) $H\|c$ obtained from $\rho_{ab}(T)$ (open symbols) and $\rho_{ab}(H)$ (closed symbols) curves. Points above 35 T were extracted by linear extrapolation of $\rho_{ab}(H)$ at $\mu_0 H < 35$ T to $\rho_{ab}(H) = 0.9\rho_{n,ab}(T_c, H)$.

limit, $\mu_0 H_{c2}(T)$ can be calculated using the following equation in terms of digamma functions:[40]

$$\ln\frac{1}{t} = \left(\frac{1}{2} + \frac{i\lambda_{so}}{4\gamma}\right)\psi\left(\frac{1}{2} + \frac{\bar{h} + \lambda_{so}/2 + i\gamma}{2t}\right)$$
$$+ \left(\frac{1}{2} - \frac{i\lambda_{so}}{4\gamma}\right)\psi\left(\frac{1}{2} + \frac{\bar{h} + \lambda_{so}/2 - i\gamma}{2t}\right) - \psi\left(\frac{1}{2}\right), \quad (2)$$

where $t = T/T_c$, $\gamma \equiv [(\alpha\bar{h})^2 - (\lambda_{so}/2)^2]^{1/2}$ and

$$h^* \equiv \frac{\bar{h}}{(-d\bar{h}/dt)_{t=1}} = \frac{\pi^2 \bar{h}}{4} = \frac{H_{c2}}{(-dH_{c2}/dt)_{t=1}}. \quad (3)$$

Here, we assume that $\lambda_{so} = 0$ because the spin-orbit scattering is expected to be rather weak[41] and the equation can be simplified as:

$$\ln\frac{1}{t} = \frac{1}{2}\psi\left[\frac{1}{2} + \frac{(1+\alpha)\bar{h}}{2t}\right] + \frac{1}{2}\psi\left[\frac{1}{2} + \frac{(1-\alpha)\bar{h}}{2t}\right] - \psi\left(\frac{1}{2}\right). \quad (4)$$

When $\alpha = 0$, in the absence of the spin-paramagnetic effect and the spin-orbit interaction, orbital limited upper critical field H_{c2}^* is described by,

$$\ln\frac{1}{t} = \psi\left(\frac{1}{2} + \frac{\bar{h}}{2t}\right) - \psi\left(\frac{1}{2}\right) \quad (5)$$

and $\mu_0 H_{c2}^*(0) = -0.693(d\mu_0 H_{c2}/dT)_{T_c} T_c$, i.e., Eq. (1).

As shown in the Fig. 6, the data points of $\mu_0 H_{c2}(T)$ for $H\|ab$ and $H\|c$ in both samples cannot be explained well using the WHH model with $\alpha = 0$ and $\lambda_{so} = 0$ [Figs. 6(a) and 6(b) solid lines] We obtain excellent fits for the $\mu_0 H_{c2,ab}(T)$ and $\mu_0 H_{c2,c}(T)$ in Figs. 6(a) and 6(b) using Eq. (4) with spin-paramagnetic effect. These results indicate that the spin-paramagnetic effect is the dominant pair-breaking mechanism in Se-39 and Se-11 for both $H\|ab$ and $H\|c$.

The paramagnetically limited field $\mu_0 H_{c2}^p(0)$ is given by $\mu_0 H_{c2}^p(0) = \mu_0 H_{c2}^*(0)/\sqrt{1+\alpha^2}$ and $\alpha = \sqrt{2}H_{c2}^*(0)/H_p(0)$, where $\mu_0 H_p(0)$ is zero-temperature Pauli limited field.[42] The calculated $\mu_0 H_{c2}^p(0)$ and $\mu_0 H_p(0)$ using α obtained from $H_{c2}(T)$ data fitting are listed in Table II. From the $\mu_0 H_{c2}(0)$ zero-temperature coherence length $\xi(0)$ can be estimated with Ginzburg-Landau formula $\mu_0 H_{c2}(0) = \Phi_0/2\pi\xi^2(0)$, where $\Phi_0 = 2.07 \times 10^{-15}$Wb (Table II). The $\mu_0 H_{c2}(0)$ [determined by $\mu_0 H_{c2}^p(0)$] of Se-39 in both field directions are close to previously reported.[43] Our results suggest that Fe(Te,Se) exhibits the spin-singlet pairing in the superconducting state. One the other hand, we also analyze our data using the two-band theory,[17,44] and the fits are unsatisfactory the two-band model (not shown here).

It is instructive to discuss the origin of enhancement of spin-paramagnetic effect, i.e., reduced values of $\mu_0 H_p(0)$. The Maki parameter α is enhanced for disordered systems.[41,45] For Se-39, more Se doping introduces more disorder than in Se-11. This effect could contribute to larger $\alpha_{H\|ab}$ of Se-39 when compared to Se-11. However, it cannot explain the inverse trend of $\alpha_{H\|c}$. Therefore another effect
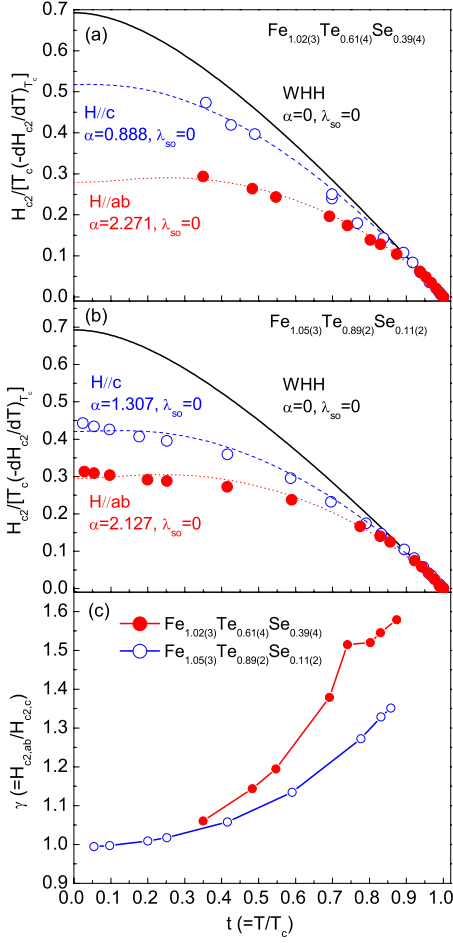
FIG. 6. (Color online) Normalized upper critical field h^* vs reduced temperature $t=T/T_c$ for (a) Se-39 and (b) Se-11 for $H\|ab$ (closed circle) and $H\|c$ (open circle). Solid lines: WHH model with $\alpha=0$, $\lambda=0$; Dotted and dash lines: fitted $h^*(t)$ including spin-paramagnetic effect for $H\|ab$ and $H\|c$, respectively. (c) The anisotropy in the upper critical field, $\gamma=H_{c2,ab}(T)/H_{c2,c}(T)$, as a function of reduced temperature $t=T/T_c$.

must compete with disorder. This may be the effect of excess Fe in Fe(2) position.

Excess Fe in Fe(2) position is the unique feature of 11-system, different from other Fe pnictide superconductors. The Fe(2) has larger local magnetic moment than Fe(1) in Fe-(Te,Se) layers. The Fe(2) moment is present even if the SDW antiferromagnetic ordering of the Fe plane is suppressed by doping or pressure, contributing to $N(E_F)$.[16] According to the expression of $\mu_0H_p(0)$ with strong coupling

correction considering e-boson and e-e interaction:[41,46,47]

$$\mu_0H_p(0) = 1.86(1+\lambda)^\varepsilon \eta_\Delta \eta_{ib}(1-I), \qquad (6)$$

where η_Δ describes the strong coupling intraband correction for the gap, I is the Stoner factor $I=N(E_F)J$, $N(E_F)$ is the electronic density of states (DOS) per spin at the Fermi level E_F, J is an effective exchange integral, η_{ib} is introduced to describe phenomenologically the effect of the gap anisotropy, λ is electron—boson coupling constant and $\varepsilon=0.5$ or 1. It can be seen that $\mu_0H_p(0)$ can decrease if the Stoner factor increases via enhancement of J or $N(E_F)$. Excess Fe in Fe(2) site with local magnetic moment could interact with itinerant electron in Fe layer, resulting in exchange enhanced Pauli paramagnetism or Ruderman-Kittel-Kasuya-Yosida (RKKY) interaction, thus enhancing J. Hence, higher content of excess Fe in Se-11, could lead to larger $\alpha_{H\|c}$ than in Se-39. Another possibility may be that the $N(E_F)$ is decreased with increasing the content of Se.[14] This trend will also enhance the Pauli limited field, i.e., suppress the spin-paramagnetic effect, according to above formula. This could be why the $\mu_0H_p(0)$ of Se-39 is higher than that of Se-11 if we assume other parameters in Eq. (6) are not changed.

Finally, we discuss the anisotropy of $\mu_0H_{c2}(T)$. The temperature dependence of anisotropy of $\mu_0H_{c2}(T)$, $\gamma[=H_{c2,ab}(T)/H_{c2,c}(T)]$, obtained from the $\mu_0H_{c2,onset}(T)$ data is shown in Fig. 6(c) as a function of reduced temperature $t=T/T_c$. The γ of Se-11 is smaller than that of Se-39. The difference in γ between the two samples decreases gradually. Both γ values decrease to about 1 with decreasing temperature, larger than in Fe(Te,S) and similar to previously reported in Fe(Te,Se).[27,43] These results show that Fe(Te,Se) is a high-field isotropic superconductor.

V. CONCLUSION

In summary, the anisotropy in the upper critical field of $Fe_{1.02(3)}Te_{0.61(4)}Se_{0.39(4)}$ and $Fe_{1.05(3)}Te_{0.89(2)}Se_{0.11(2)}$ single crystals was studied in high and stable magnetic fields up to 35 T. It is found that the zero-temperature upper critical field is much smaller than the predicted result of WHH theory without the spin-paramagnetic effect. The anisotropy of the upper critical field decreases with decreasing temperature, becoming nearly isotropic at low temperature. The spin-paramagnetic effect is the dominant pair-breaking mechanism for both of $H\|ab$ and $H\|c$.

TABLE II. Superconducting parameters of Se-39 and Se-11 obtained from the analysis of $\mu_0H_{c2,onset}(T)$. $\mu_0H_{c2}^*(0)$, $\mu_0H_{c2}^p(0)$, and $\mu_0H_p(0)$ are the zero-temperature orbital, paramagnetically, and Pauli limited upper critical fields, respectively. α is the fitted Maki parameter ($\lambda_{so}=0$). $\xi_{ab}(0)$ and $\xi_c(0)$ are the ab-plane and c-axis zero-temperature coherence length calculated using $\mu_0H_{c2}^p(0)$, respectively.

	$\mu_0H_{c2,ab}^*(0)$ (T)	$\mu_0H_{c2,c}^*(0)$ (T)	$\mu_0H_{c2,ab}^p(0)$ (T)	$\mu_0H_{c2,c}^p(0)$ (T)	$\mu_0H_{p,ab}(0)$ (T)	$\mu_0H_{p,c}(0)$ (T)	$\alpha_{H\|ab}$	$\alpha_{H\|c}$	$\xi_{ab}(0)$ (nm)	$\xi_c(0)$ (nm)
$Fe_{1.02(3)}Te_{0.61(4)}Se_{0.39(4)}$	98.8	57.9	39.8	43.3	61.5	92.2	2.271	0.888	2.76	3.00
$Fe_{1.05(3)}Te_{0.89(2)}Se_{0.11(2)}$	83.1	59.0	35.4	35.9	55.3	63.8	2.127	1.307	3.03	3.07

---

*Present address: Ames Laboratory U.S. DOE and Department of Physics and Astronomy, Iowa State University, Ames, IA 50011, USA.

[1] Y. Kamihara, T. Watanabe, M. Hirano, and H. Hosono, J. Am. Chem. Soc. **130**, 3296 (2008).

[2] X. H. Chen, T. Wu, G. Wu, R. H. Liu, H. Chen, and D. F. Fang, Nature (London) **453**, 761 (2008).

[3] G. F. Chen, Z. Li, D. Wu, G. Li, W. Z. Hu, J. Dong, P. Zheng, J. L. Luo, and N. L. Wang, Phys. Rev. Lett. **100**, 247002 (2008).

[4] Z. A. Ren, J. Yang, W. Lu, Y. Wei, X. L. Shen, Z. C. Li, G. C. Che, X. L. Dong, L. L. Sun, F. Zhou, and Z. X. Zhao, EPL **82**, 57002 (2008).

[5] H.-H. Wen, G. Mu, L. Fang, H. Yang, and X. Y. Zhu, EPL **82**, 17009 (2008).

[6] M. Rotter, M. Tegel, and D. Johrendt, Phys. Rev. Lett. **101**, 107006 (2008).

[7] G.-F. Chen, Z. Li, G. Li, W.-Z. Hu, J. Dong, J. Zhou, X.-D. Zhang, P. Zheng, N.-L. Wang, and J.-L. Luo, Chin. Phys. Lett. **25**, 3403 (2008).

[8] X. C. Wang, Q. Q. Liu, Y. X. Lv, W. B. Gao, L. X. Yang, R. C. Yu, F. Y. Li, and C. Q. Jin, Solid State Commun. **148**, 538 (2008).

[9] H. Ogino, Y. Matsumura, Y. Katsura, K. Ushiyama, S. Horii, K. Kishio, and J. Shimoyama, Supercond. Sci. Technol. **22**, 075008 (2009).

[10] X. Y. Zhu, F. Han, G. Mu, P. Cheng, B. Shen, B. Zeng, and H.-H. Wen, Phys. Rev. B **79**, 220512(R) (2009).

[11] F. C. Hsu, J. Y. Luo, K. W. Yeh, T. K. Chen, T. W. Huang, P. M. Wu, Y. C. Lee, Y. L. Huang, Y. Y. Chu, D. C. Yan, and M. K. Wu, Proc. Natl. Acad. Sci. U.S.A. **105**, 14262 (2008).

[12] K.-W. Yeh, T. W. Huang, Y. L. Huang, T. K. Chen, F. C. Hsu, P. M. Wu, Y. C. Lee, Y. Y. Chu, C. L. Chen, J. Y. Luo, D. C. Yan, and M. K. Wu, EPL **84**, 37002 (2008).

[13] Y. Mizuguchi, F. Tomioka, S. Tsuda, T. Yamaguchi, and Y. Takano, Appl. Phys. Lett. **94**, 012503 (2009).

[14] A. Subedi, L. Zhang, D. J. Singh, and M. H. Du, Phys. Rev. B **78**, 134514 (2008).

[15] Y. Mizuguchi, F. Tomioka, S. Tsuda, T. Yamaguchi, and Y. Takano, Appl. Phys. Lett. **93**, 152505 (2008).

[16] L. J. Zhang, D. J. Singh, and M. H. Du, Phys. Rev. B **79**, 012506 (2009).

[17] J. Jaroszynski, F. Hunte, L. Balicas, Y.-J. Jo, I. Raičević, A. Gurevich, D. C. Larbalestier, F. F. Balakirev, L. Fang, P. Cheng, Y. Jia, and H. H. Wen, Phys. Rev. B **78**, 174523 (2008).

[18] F. Hunte, J. Jaroszynski, A. Gurevich, D. C. Larbalestier, R. Jin, A. S. Sefat, M. A. McGuire, B. C. Sales, D. K. Christen, and D. Mandrus, Nature (London) **453**, 903 (2008).

[19] H.-S. Lee, M. Bartkowiak, J.-H. Park, J.-Y. Lee, J.-Y. Kim, N.-H. Sung, B. K. Cho, C.-U. Jung, J. S. Kim, and H.-J. Lee, Phys. Rev. B **80**, 144512 (2009).

[20] H. Q. Yuan, J. Singleton, F. F. Balakirev, S. A. Baily, G. F. Chen, J. L. Luo, and N. L. Wang, Nature (London) **457**, 565 (2009).

[21] S. A. Baily, Y. Kohama, H. Hiramatsu, B. Maiorov, F. F. Balakirev, M. Hirano, and H. Hosono, Phys. Rev. Lett. **102**, 117004 (2009).

[22] M. M. Altarawneh, K. Collar, C. H. Mielke, N. Ni, S. L. Bud'ko, and P. C. Canfield, Phys. Rev. B **78**, 220505(R) (2008).

[23] M. Kano, Y. Kohama, D. Graf, F. Balakirev, A. S. Sefat, M. A. Mcguire, B. C. Sales, D. Mandrus, and S. W. Tozer, J. Phys. Soc. Jpn. **78**, 084719 (2009).

[24] T. Terashima, M. Kimata, H. Satsukawa, A. Harada, K. Hazama, S. Uji, H. Harima, G.-F. Chen, J.-L. Luo, and N.-L. Wang, J. Phys. Soc. Jpn. **78**, 063702 (2009).

[25] T. Kida, T. Matsunaga, M. Hagiwara, Y. Mizuguchi, Y. Takano, and K. Kindo, J. Phys. Soc. Jpn. **78**, 113701 (2009).

[26] B. Hunter, "Rietica-A visual Rietveld program," International Union of Crystallography Commission on Powder Diffraction Newsletter No. 20, (Summer) http://www.rietica.org (1998).

[27] R. W. Hu, E. S. Bozin, J. B. Warren, and C. Petrovic, Phys. Rev. B **80**, 214514 (2009).

[28] G. F. Chen, Z. G. Chen, J. Dong, W. Z. Hu, G. Li, X. D. Zhang, P. Zheng, J. L. Luo, and N. L. Wang, Phys. Rev. B **79**, 140509(R) (2009).

[29] Z.-S. Wang, H.-Q. Luo, C. Ren, and H.-H. Wen, Phys. Rev. B **78**, 140501(R) (2008).

[30] Z. Bukowski, S. Weyeneth, R. Puzniak, P. Moll, S. Katrych, N. D. Zhigadlo, J. Karpinski, H. Keller, and B. Batlogg, Phys. Rev. B **79**, 104521 (2009).

[31] J. Karpinski, N. D. Zhigadlo, S. Katrych, Z. Bukowski, P. Moll, S. Weyeneth, H. Keller, R. Puzniak, M. Tortello, D. Daghero, R. Gonnelli, I. Maggio-Aprile, Y. Fasano, Ø. Fischer, K. Rogacki, and B. Batlogg, Physica C **469**, 370 (2009).

[32] W. K. Kwok, S. Fleshler, U. Welp, V. M. Vinokur, J. Downey, G. W. Crabtree, and M. M. Miller, Phys. Rev. Lett. **69**, 3370 (1992).

[33] W. K. Kwok, J. Fendrich, S. Fleshler, U. Welp, J. Downey, and G. W. Crabtree, Phys. Rev. Lett. **72**, 1092 (1994).

[34] H. Safar, P. L. Gammel, D. A. Huse, D. J. Bishop, J. P. Rice, and D. M. Ginsberg, Phys. Rev. Lett. **69**, 824 (1992).

[35] G. Blatter, M. V. Feigel'man, V. B. Geshkenbein, A. I. Larkin, and V. M. Vinokur, Rev. Mod. Phys. **66**, 1125 (1994).

[36] Z. Pribulova, T. Klein, J. Kacmarcik, C. Marcenat, M. Konczykowski, S. L. Bud'ko, M. Tillman, and P. C. Canfield, Phys.

Rev. B **79**, 020508(R) (2009).

[37] B. C. Sales, A. S. Sefat, M. A. McGuire, R. Y. Jin, D. Mandrus, and Y. Mozharivskyj, Phys. Rev. B **79**, 094521 (2009).

[38] T. J. Liu, X. Ke, B. Qian, J. Hu, D. Fobes, E. K. Vehstedt, H. Pham, J. H. Yang, M. H. Fang, L. Spinu, P. Schiffer, Y. Liu, and Z. Q. Mao, Phys. Rev. B **80**, 174509 (2009).

[39] W. Bao, Y. Qiu, Q. Huang, M. A. Green, P. Zajdel, M. R. Fitzsimmons, M. Zhernenkov, S. Chang, M. H. Fang, B. Qian, E. K. Vehstedt, J. H. Yang, H. M. Pham, L. Spinu, and Z. Q. Mao, Phys. Rev. Lett. **102**, 247001 (2009).

[40] N. R. Werthamer, E. Helfand, and P. C. Hohenberg, Phys. Rev. **147**, 295 (1966).

[41] G. Fuchs, S.-L. Drechsler, N. Kozlova, M. Bartkowiak, J. E. Hamann-Borrero, G. Behr, K. Nenkov, H.-H. Klauss, H. Maeter, A. Amato, H. Luetkens, A. Kwadrin, R. Khasanov, J. Freudenberger, A. Köhler, M. Knupfer, E. Arushanov, H. Rosner,

B. Büchner, and L. Schultz, New J. Phys. **11**, 075007 (2009).

[42] K. Maki, Phys. Rev. **148**, 362 (1966).

[43] M. Fang, J. Yang, F. Balakirev, Y. Kohama, J. Singleton, B. Qian, Z. Mao, H. Wang, and H. Yuan, Phys. Rev. B **81**, 020509 (2010).

[44] A. Gurevich, Phys. Rev. B **67**, 184515 (2003).

[45] G. Fuchs, S.-L. Drechsler, N. Kozlova, G. Behr, A. Köhler, J. Werner, K. Nenkov, C. Hess, R. Klingeler, J. E. Hamann-Borrero, A. Kondrat, M. Grobosch, A. Narduzzo, M. Knupfer, J. Freudenberger, B. Büchner, and L. Schultz, Phys. Rev. Lett. **101**, 237003 (2008).

[46] T. P. Orlando, E. J. McNiff, Jr., S. Foner, and M. R. Beasley, Phys. Rev. B **19**, 4545 (1979).

[47] M. Schossmann and J. P. Carbotte, Phys. Rev. B **39**, 4210 (1989).